INSTIITUTE OF ACCELERATING SYSTEMS AND APPLICATIONS, ATHENS, GREECE
WP10 Coordinator

MEDITERRANEAN OCEAN FORECASTING SYSTEM: TOWARD ENVIRONMENTAL PREDICTION

MFSTEP

Project Deliverable Report D9

WP10: Atmospheric Forcing and Air-Sea Interaction Studies

Project title	**MEDITERRANEAN OCEAN FORECASTING SYSTEM: TOWARD ENVIRONMENTAL PREDICTION**					
Project acronym	**MFSTEP**					
Contract number	**EVK3-CT-2002-00075**					
Deliverable number	**D9**					
Deliverable title	**Atmospheric simulations with high resolution SSTs**					
Work package	**WP10 Atmospheric Forcing and Air-Sea Interaction Studies**					
Name of WP10 Coordinator	**Prof. George Kallos Institute of Accelerating Systems and Applications, Athens, Greece**					
Date of delivery	**February 28, 2005**					
Report status		**Draft**		**Final**	**X**	
Project home page	**http://www.bo.ingv.it/mfstep/**					
WP10 home page	**http://forecast.uoa.gr/mfstep/**					

1 Introduction

This report describes the work performed by IASA and UAT under the scopes of deliverable 9 (subtask 10210) of WP10. This work package contains the necessary activities to create and deliver the atmospheric surface fields to the WP8 and WP9 ocean modelling community, to perform the Scientific Validation Period (SVP) intercomparison of atmospheric models and to study the sensitivity of the atmosphere to sea surface conditions. The aim of this sub-task (deliverable 9) is to implement the high-resolution SSTs of WP3 in SKIRON/Eta model and to study their influence on the atmospheric flow regimes.

2 The high-resolution SSTs

A high-resolution satellite SST dataset was produced in the framework of WP3 and it became available to the partners of subtask 10210 in order to be implemented in SKIRON/Eta model (LAM2). The horizontal resolution of this dataset is 1/16° x 1/16° (longitude-latitude) which is equivalent to about 5.5-6 km in our area of interest. These SSTs were expected to represent the spatial variability of the sea-surface temperatures in the Mediterranean Sea more accurately than the 0.5x0.5 degrees operational SSTs.

2.1 Description

The high-resolution SSTs were available in daily files in Netcdf format from 19 May 2004 to 31 January 2005. The first dataset became available in the beginning of August 2004. Operational SSTs at a resolution of 0.5x0.5 degrees were also available for the same period allowing the intercomparison of the two datasets and the investigation of their influence on atmospheric forecasts.

The domain of the high-resolution satellite SSTs extended from 18.125°W to 36.25°E and from 30.25°N to 46°N. The SSTs of 13 October 2004 at the original resolution (1/16°x1/16°) for the entire domain that became available by WP3 appears in Figure 1. Similarly Figure 2 presents the same SST field zoomed over Greece. It is obvious that the new dataset provides significant details about the spatial variability of SSTs in the Mediterranean Sea and Eastern Atlantic ocean. However, there is lack of data in a number of seas, such as the Black Sea, the Red Sea, the Vosporos Straits, as well as in various areas near the coastline and in the lakes. These regions should be analyzed by the high-resolution of this product. Moreover, the domain of the high-resolution SSTs is smaller than the computational domain of the operational SKIRON/Eta modeling system (LAM2) that extends from 24.38°N to 51°N and from 21.04°W to 51.04°E.

The above analysis shows that the new product is likely to provide significant information about the SST patterns in our area of interest, but, is also needs further pre-processing before it is utilized by SKIRON/Eta model.

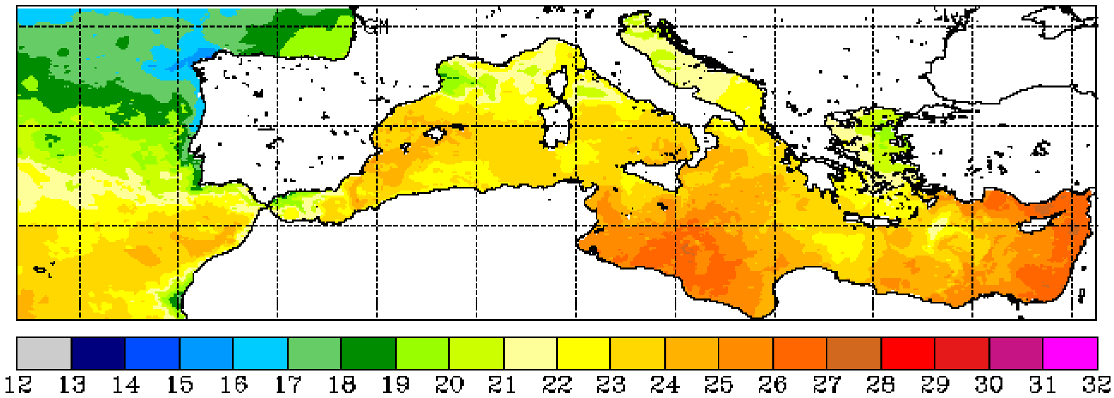

Figure 1. *The high-resolution SSTs (1/16°x1/16°) of 13 October 2004 in the entire domain provided by MFSTEP-WP3. Units: °C.*

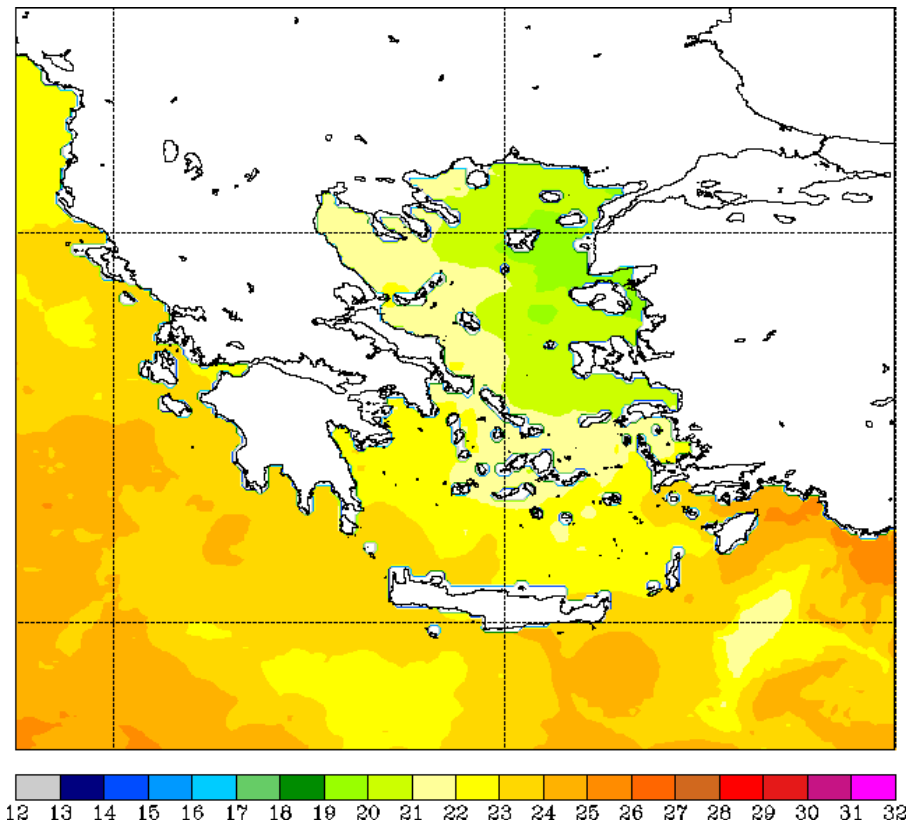

Figure 2. *The high-resolution SSTs (1/16°x1/16°) of 13 October 2004 focused over Greece. Units: °C.*

2.2 Implementation in SKIRON/Eta

The influence of the high-resolution SSTs on the atmospheric flow regimes was studied using the SKIRON/Eta modeling system. The SSTs were firstly decoded from the original Netcdf format and then they were interpolated into the E-grid of the operational model domain. In the development of the pre-processing algorithms, special attention was given in the calculation of the SSTs near the coastline.

Figure 3a shows the SST field of Figure 1 interpolated into the E-grid of the operational SKIRON/Eta domain. The horizontal resolution of the E-grid is 0.1°x0.1°. Despite the fact that the SSTs are interpolated into a grid with horizontal resolution coarser than that of the original dataset, no loss of information is observed. This happens because the two resolutions (0.1° and 1/16°) do not differ significantly. Moreover, the lack of SSTs in several regions of the domain is obvious. The operational SSTs (Figure 3b) were used in data void regions because the atmospheric numerical models require full meteorological fields in the initial conditions.

Subjective analysis and special algorithms allowed the identification of cases with unrealistically sharp gradients in regions where both datasets were used. Only a few such cases appeared in the TOP period and were not used for model initialization. Figure 4 illustrates an example of the final SST product that resulted from the combination of the SSTs of Figure 3a and 3b and was used for the initialization of SKIRON/Eta on 13 October 2004. Similarly combined fields were used to initialize SKIRON/Eta in the experiments of MFSTEP subtask 10210.

2.3 SST intercomparison

The high-resolution and the operational SSTs were both available for a period of about 8 months (19 May 2004 – 31 January 2005) allowing their statistical intercomparison and the identification of any major differences. The high-resolution dataset contains detailed information about the spatiotemporal variability of the SSTs in the Mediterranean while the operational SSTs are widely used worldwide and have been shown to improve weather forecasting. Thiebaux et al. (2003) showed that their use by ETA model resulted to improved forecasts of storm track and precipitation over Eastern US.

The intercomparison was performed on a common grid using some well-known statistical tests. Both SSTs were firstly interpolated into the 0.1°x0.1° E-grid of the operational SKIRON/Eta domain and the statistical methods were applied on the grid-points that both datasets were valid.

A total of 15556 grid-points (over sea) was used. The differences of the SSTs were investigated using monthly-mean values of the differences (equation 1) and the absolute differences (equation 2). The corresponding formulae for each grid-point are:

$$\text{Mean Difference} = \frac{\sum_{i=1}^{n}(SST_H^i - SST_C^i)}{n} \qquad \text{(equation 1)}$$

and

$$\text{Mean Absolute Difference} = \frac{\sum_{i=1}^{n}\left|SST_H^i - SST_C^i\right|}{n} \qquad \text{(equation 2)}$$

where n is the number of the days that both datasets were available at each month, SST_H^i is the high-resolution SST of the i day (interpolated in the 0.1°x0.1° E-grid) and SST_C^i is the coarser-resolution operational SST of the i day (interpolated in the 0.1°x0.1° E-grid).

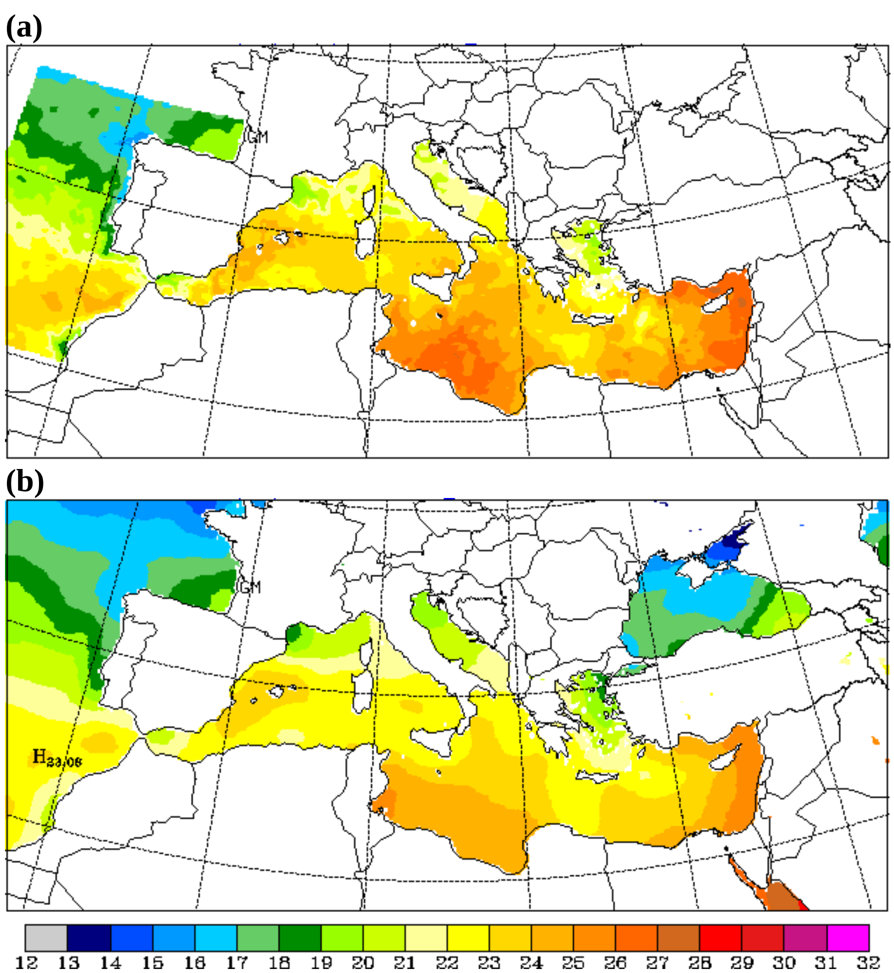

Figure 3. *a) The high-resolution and b) the operational SSTs interpolated into the 0.1°x0.1° E-grid of the operational SKIRON/Eta domain on 13 October 2004. Units: °C.*

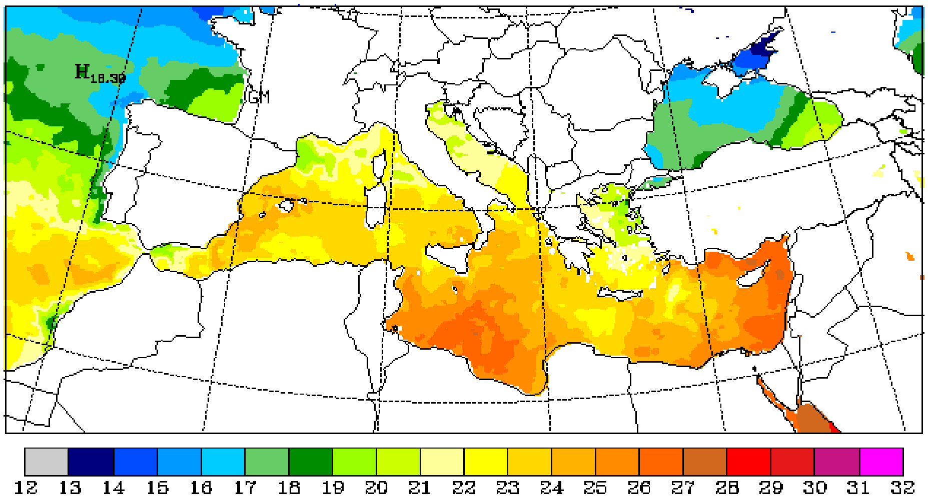

Figure 4. *The SSTs that resulted from the combination of the high-resolution and the operational SSTs and were used to initialize SKIRON/Eta on 13 October 2004. Units: °C.*

The two datasets generally exhibited small differences in the Mediterranean Sea with values less than 0.5°C (Figure 5). The high-resolution satellite dataset provided colder SSTs than the operational set in June, July, December 2004 and January 2005, while warmer values were estimated from August to November 2004. Maximum warm (cold) anomalies appeared in October and November (June), but generally they did not exceed 1°C. Larger differences appeared only locally and they were located close to coastline. This was probably due to the fact that the high-resolution SSTs were able to analyze local effects more accurately than the coarser operational SSTs. An example is the SST cooling next to the west coast of Portugal and Morocco which is likely to be caused by upwelling because of the strong winds (also see Figure 3a, b). Another possible reason for the existence of localized maximum (minimum) SST differences next to the coastline is the use of difference land-sea masks in the calculation of the SSTs.

A more robust statistical measure of the differences between the two SSTs is the mean of their absolute differences (equation 2). Examination of the mean monthly charts of Figure 6 shows that in general the absolute differences were smaller than 0.8-1°C. Similarly to the mean differences, larger mean absolute differences appear locally (mainly next to the coastline). The two datasets were similar in December 2004 (Figure 6g) and January 2005 (Figure 6h) when the mean absolute differences were smaller than 0.4°C. The above results are summarized in Table 1 that presents the mean difference and the mean absolute difference averaged over the SKIRON/Eta grid-points that both datasets were valid (15556 grid-points). Positive mean differences indicate warmer SSTs in the high-resolution satellite dataset.

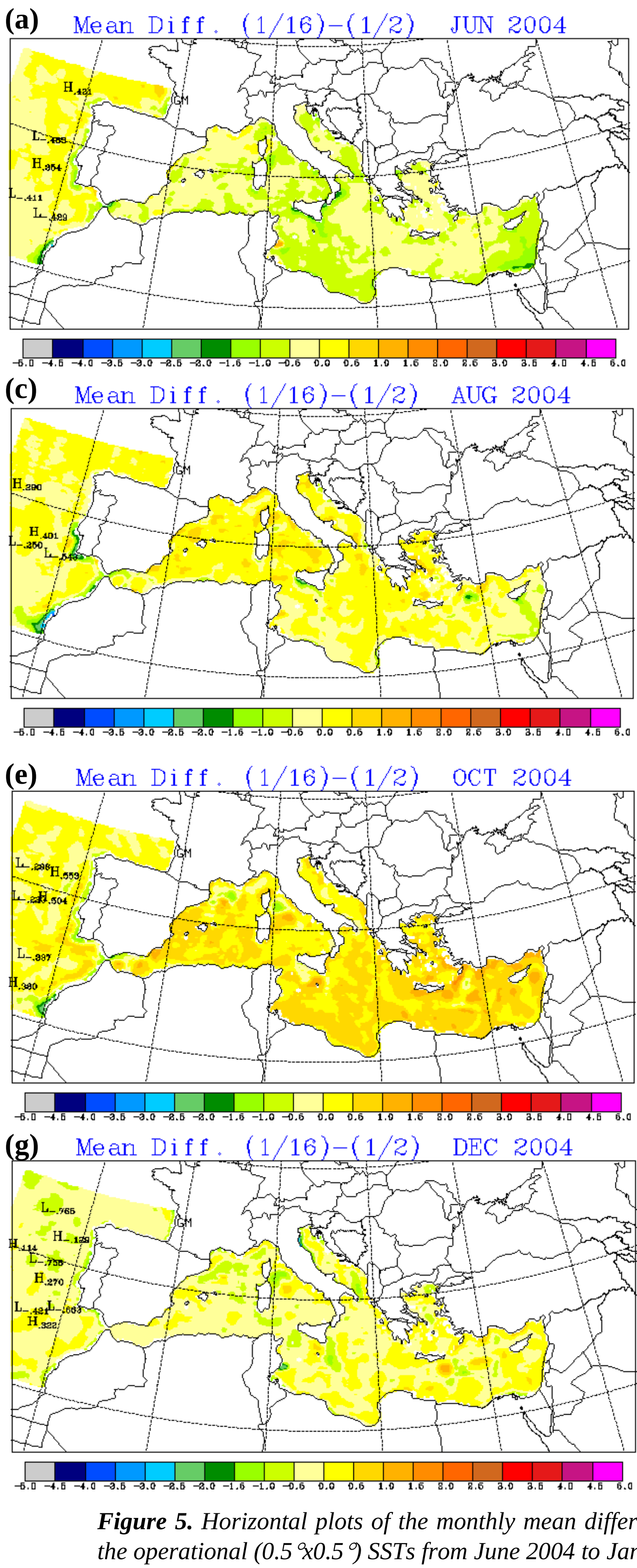

Figure 5. *Horizontal plots of the monthly mean difference between the high-resolution (1/16°x1/16°) and the operational (0.5°x0.5°) SSTs from June 2004 to January 2005. Units: °C.*

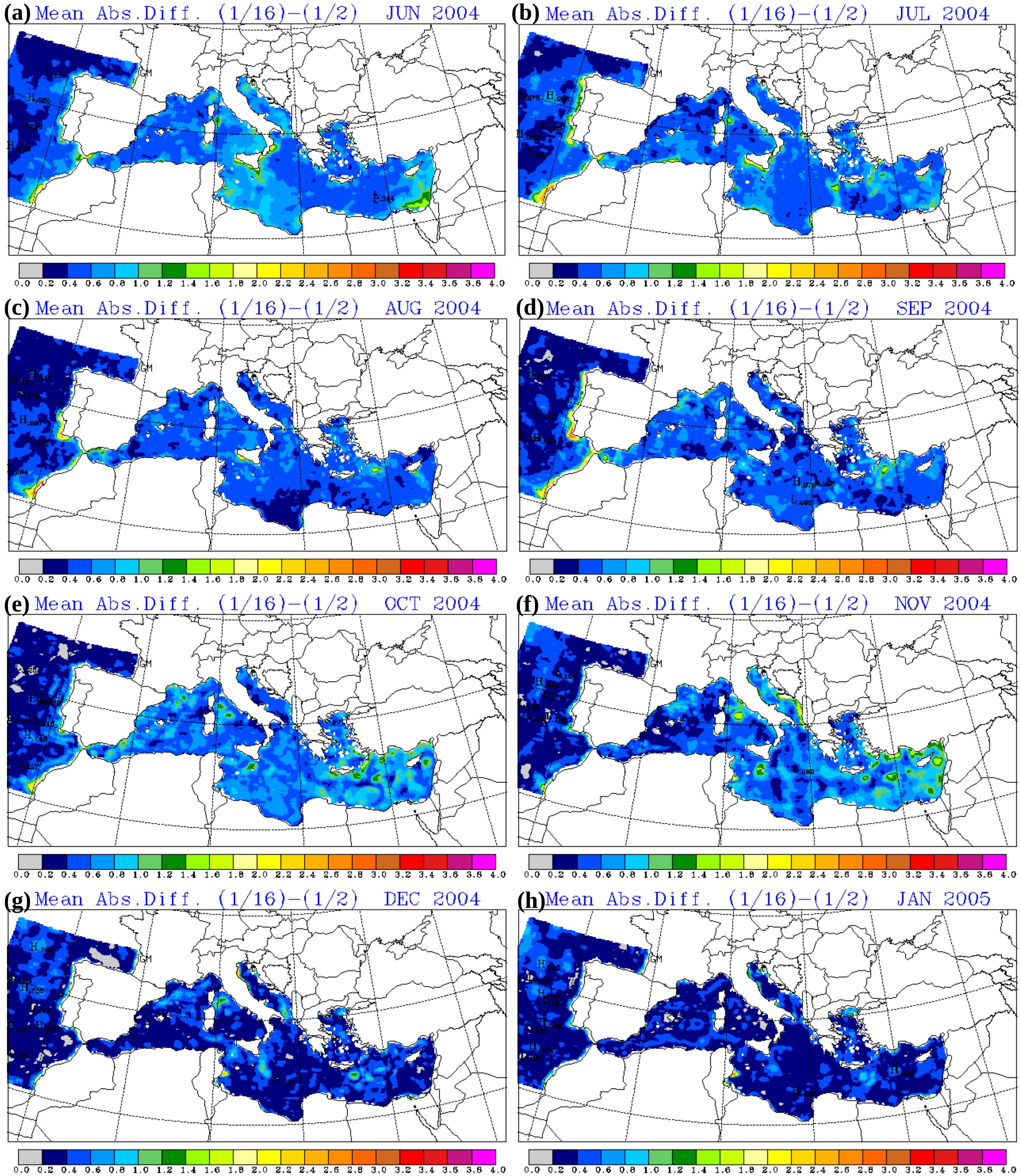

Figure 6. *Horizontal plots of the monthly mean absolute difference between the high-resolution (1/16°x1/16°) and the operational SSTs (0.5°x0.5°) from June 2004 to January 2005. Units: °C.*

Month	Days with valid data	Mean Difference	Mean Absolute Difference	Mean Standard Deviation	
				High-resolution	Operational
June 2004	29	-0.333	0.587	1.394	1.313
July 2004	29	-0.222	0.566	0.777	0.753
August 2004	31	0.029	0.489	0.626	0.556
September 2004	28	0.097	0.504	0.641	0.697
October 2004	30	0.336	0.552	0.71	0.729
November 2004	28	0.242	0.54	1.089	1.047
December 2004	31	-0.167	0.388	0.654	0.637
January 2005	31	-0.13	0.375	0.499	0.536

Table 1. *The monthly mean differences, absolute differences and standard deviation of the high-resolution and the operational SST datasets from June 2004 to January 2005, averaged over the SKIRON/Eta grid-points that both datasets were valid (15556 grid-points). Positive differences indicate warmer SSTs in the high-resolution satellite dataset. Units: ℃.*

The two SST datasets also exhibited significant similarities in their monthly variability. Figure 7 presents the standard deviation of each dataset for each month from June 2004 to January 2005. The standard deviation values appear to follow similar patterns. The regions with the strongest and weakest variability at each month are the same in the two SSTs and the extreme values are comparable. The fact that the satellite SST deviation is more detailed than the operational one is due to its finer resolution. The strongest SST variability occurs in the transitional period (June and November) while the weakest variability appears in summer (August) and winter (January) as expected. In agreement with the above results, Table 1 shows that the difference in the monthly mean standard deviation (averaged over all the grid-points that both datasets were valid) is less than 0.1°C.

In summary, the analysis of this section showed that the procedures followed by CNR and NCEP in order to derive the high-resolution and the operational SSTs (respectively) resulted in similar products. The absolute difference showed that the two SSTs do not differ significantly. Also there was no clear indication about any systematic overestimation (or underestimation) of the SSTs by any originating center. More significantly, the spatiotemporal variability of the SSTs exhibited similar characteristics. Concluding, it seems that the two datasets are not likely to provide very different forcing in the SKIRON/Eta forecasts. In the analysis of the next section the influence of the high-resolution SSTs in synoptic and mainly in local scales will be investigated.

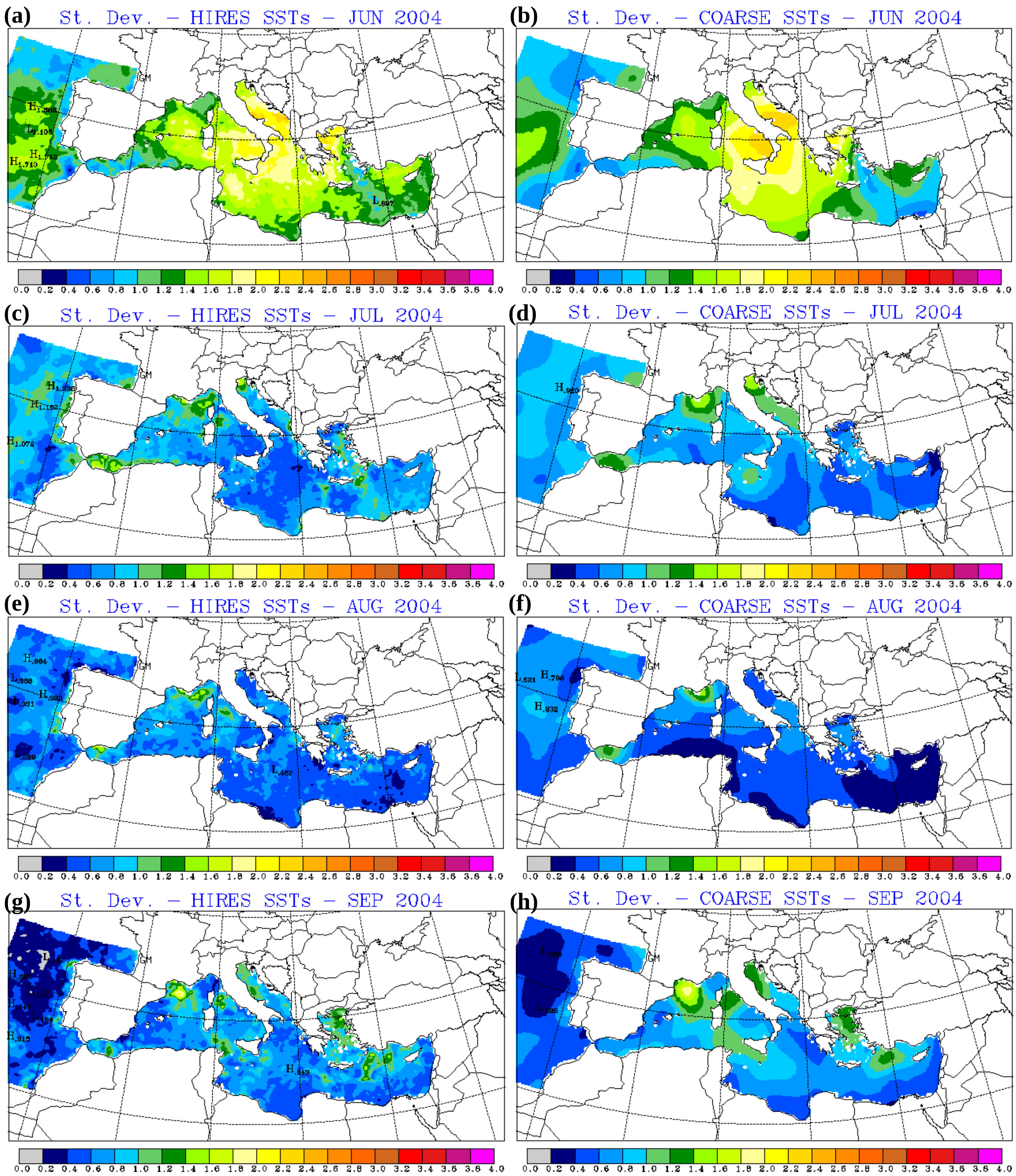

Figure 7. *Horizontal plots of the monthly mean standard deviation of the high-resolution (HIRES; panels a, c, e, g, i, k, m, o) and the operational (COARSE; panels b, d, f, h, j, l, n, p) SSTs from June 2004 to January 2005. Units: ℃.*

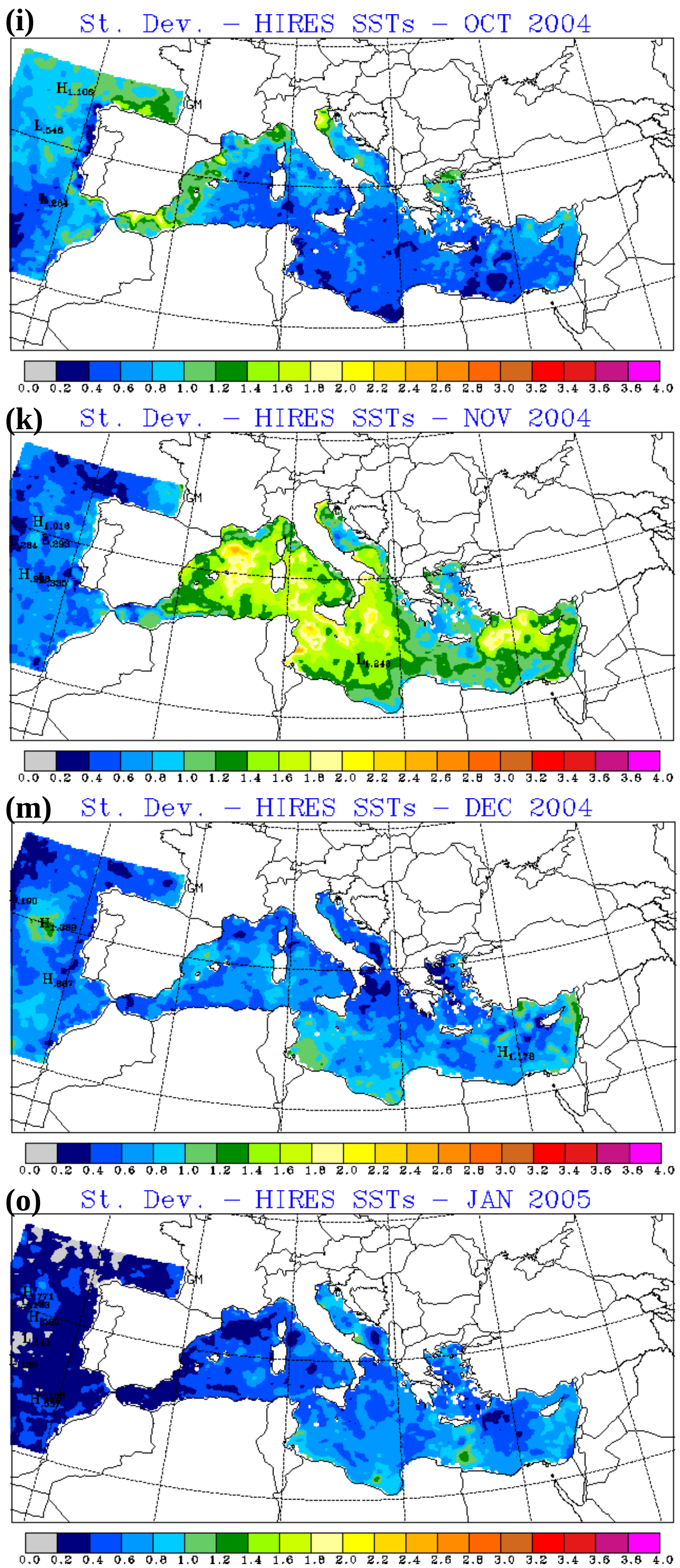

Figure 7. *(Continued)*

3 Experimental setup

The intercomparison of section 2.3 showed that the high-resolution and the operational SSTs do not differ significantly. Day-by-day analysis of the SST differences resulted in the same conclusion, but it also allowed the identification of the days in which the two datasets differ significantly. A number of these days (from June 2004 to January 2005) was selected for the sensitivity experiments of subtask 10210.

The main criteria for selecting these cases were: a) the existence of significant weather in the Mediterranean basin, b) the existence of significant SST differences between the two datasets, and c) the chosen days to be among those used for the initialization of the TOP runs. The third criterion was set because Meteo-France boundary conditions suitable for 120-hour runs existed only for the TOP cases (which are initialized every Wednesday at 0000 UTC).

Following the above criteria, seven cases were selected for sensitivity experiments. The initial time of these runs and their duration are presented in Table 2. The SST differences between the high-resolution and the operational SSTs are illustrated in Figure 8. A variety of cases was chosen, with the high-resolution SSTs to be either warmer (e.g. Figure 8c) or colder (e.g. Figure 8b) than the operational SSTs. In some cases, dipoles of warm-cold SST anomalies occurred (Figure 8f).

Initial Time		**Forecast Horizon**
Date	**Time (UTC)**	**(hours)**
14 July 2004	0000	120
21 July 2004	0000	120
13 October 2004	0000	72
3 November 2004	0000	72
17 November 2004	0000	120
5 January 2005	0000	120
19 January 2005	0000	120

Table 2. *The initial time and the duration of the SKIRON/Eta hindcasts of subtask 10210.*

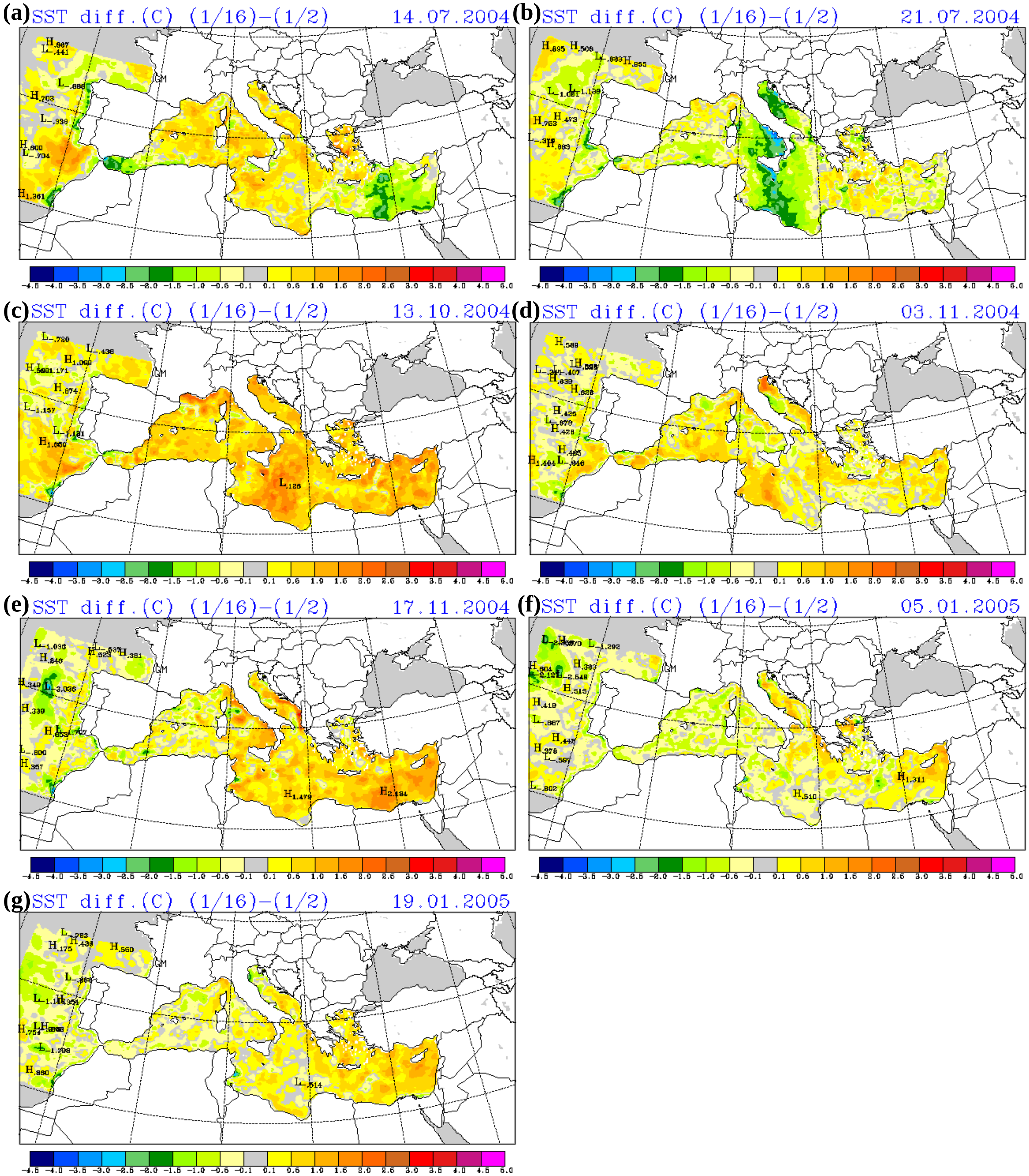

Figure 8. *Horizontal plots of the difference between the high-resolution (1/16°x1/16°) and the operational (0.5°x0.5°) SSTs on a) 14 July 2004, b) 21 July 2004, c) 13 October 2004, d) 3 November 2004, e) 17 November 2004, f) 5 January 2005, and g) 19 January 2005. Units: °C.*

The weather conditions during the selected periods covered the typical weather types (Varinou 2000) that appear in the Mediterranean from June to January. The weather patterns that prevailed in the sensitivity experiments include the Etesians, strong winds in the Gulf of Leon, transient depressions originating in the Gulf of Genova or near the Atlas mountains or in the Cyprus region, cold-air advection associated with convective activity, cold fronts associated with low-pressure centers over Europe that extend into the Mediterranean, and summertime thunderstorm activity.

Two simulations were performed for each selected case. In the first one the SKIRON/Eta model was integrated using the operational SSTs and a setup similar to TOP. The TOP setup is described in deliverable D4 of MFSTEP-WP10. The ARPEGE fields were used as initial and lateral boundary conditions. The only difference relative to the TOP runs was that here the soil moisture and temperature were initialized using the values of the global model (cold-start). In the TOP runs the soil moisture and temperature were initialized through a "warm-start" using the predicted values from the previous model cycle. In the other set of simulations, the high-resolution SSTs were utilized. No other changes were made to the setup of the model and the soil properties were initialized through a "cold-start". Therefore, the only difference of the runs performed for each selected case was the SST field. The SSTs remained fixed to their initial value throughout the simulations.

4 Model results

The outputs of the two abovementioned sets of simulations were intercompared in order to study the effects of the high-resolution SSTs on atmospheric predictions. Firstly, the model results were examined using a case study approach. It was shown in Figure 8 that significant SST anomalies existed in the selected cases. This was expected to lead to well-defined anomalies in the atmospheric predictions and to make more enlightening the influence of the high-resolution SST on the atmosphere.

4.1 Case studies

The case studies generally did not reveal large differences in the model prediction due to the use of the high-resolution SSTs. Noticeable anomalies appeared in a few cases in which strong systems were located over significant SST anomalies. Two well-defined cases will be presented here and the influence of the high-resolution SSTs on model predictions will be investigated.

4.1.1 Frontal zone in Western Greece

A frontal zone was located over western Greece on 13-14 October 2004 (Figure 9) and it was associated with heavy rain, thunderstorm activity and strong winds. In this period the high-resolution SST were up to about 1.5°C warmer than the operational SSTs in the region west of Greece (Figure 8c). The influence of the high-resolution SSTs on the evolution of the frontal zone is investigated here.

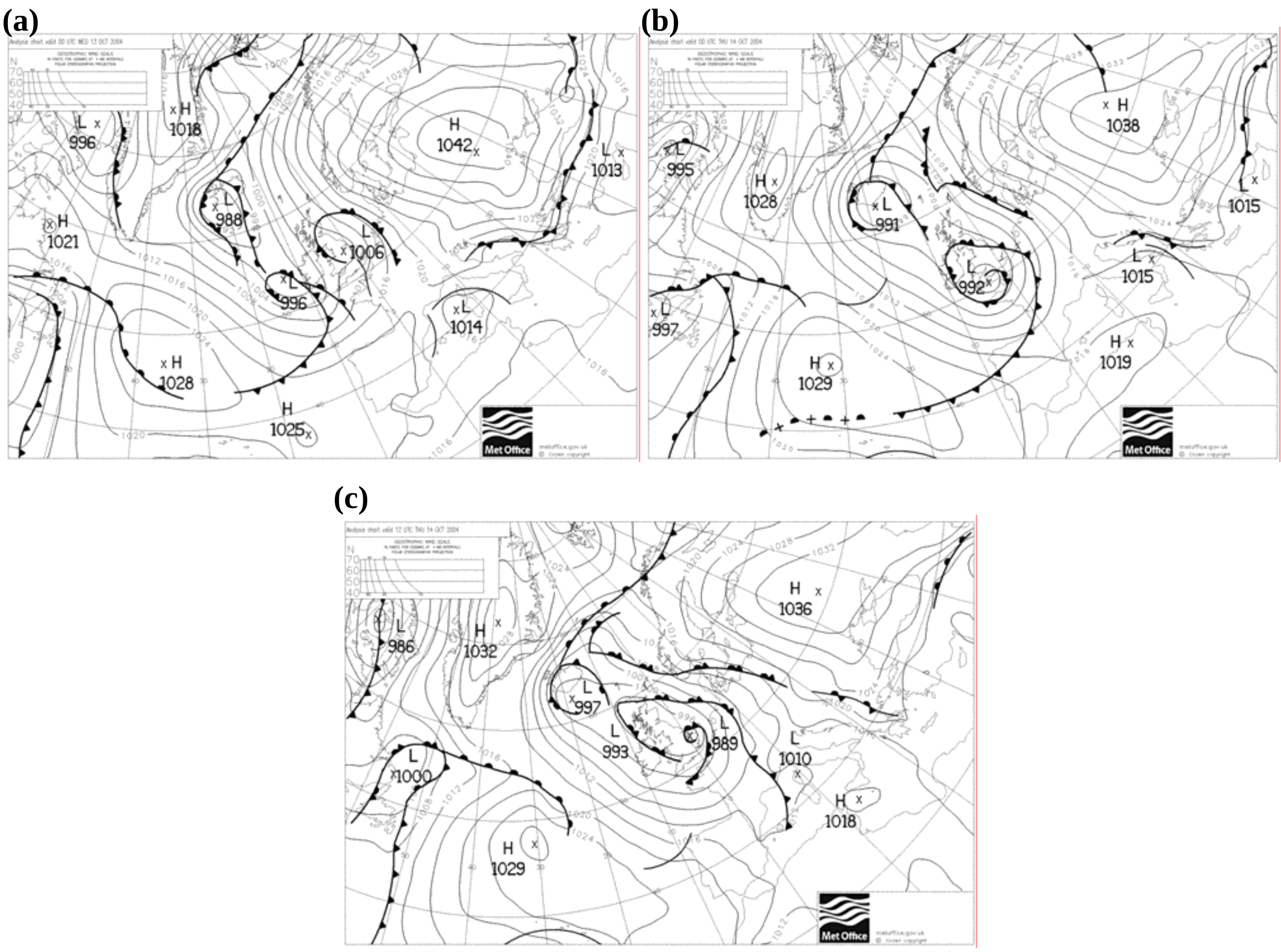

Figure 9. UKMO mean sea-level pressure (hPa) analysis charts at a) 0000 UTC 13 October 2004, b) 000 UTC 14 October 2004 and c) 1200 UTC 14 October 2004.

Figure 10 shows that the evolution of the frontal zone was predicted by SKIRON/Eta in agreement with the observations (Figure 9). Stronger precipitation was predicted in the run with the high-resolution SSTs (Figure 10a, b). It seems that the SSTs influenced not only the strength of the rainband, but also its transition speed. The rainband appears to move faster in the high-resolution SST run than in the run with the operational SSTs (Figure 10c, d). Similar changes appear in the transition speed of all the main rainbands in the model domain (Figure 11). The occurrence of stronger precipitation in the run with the (warmer) high-resolution SST is due to the stronger surface fluxes (Figure 12) that impose a stronger destabilization in the boundary layer of the storms. However, the mechanism that the surface differences (imposed by the different SSTs) alter the speed of the rainbands needs further investigation.

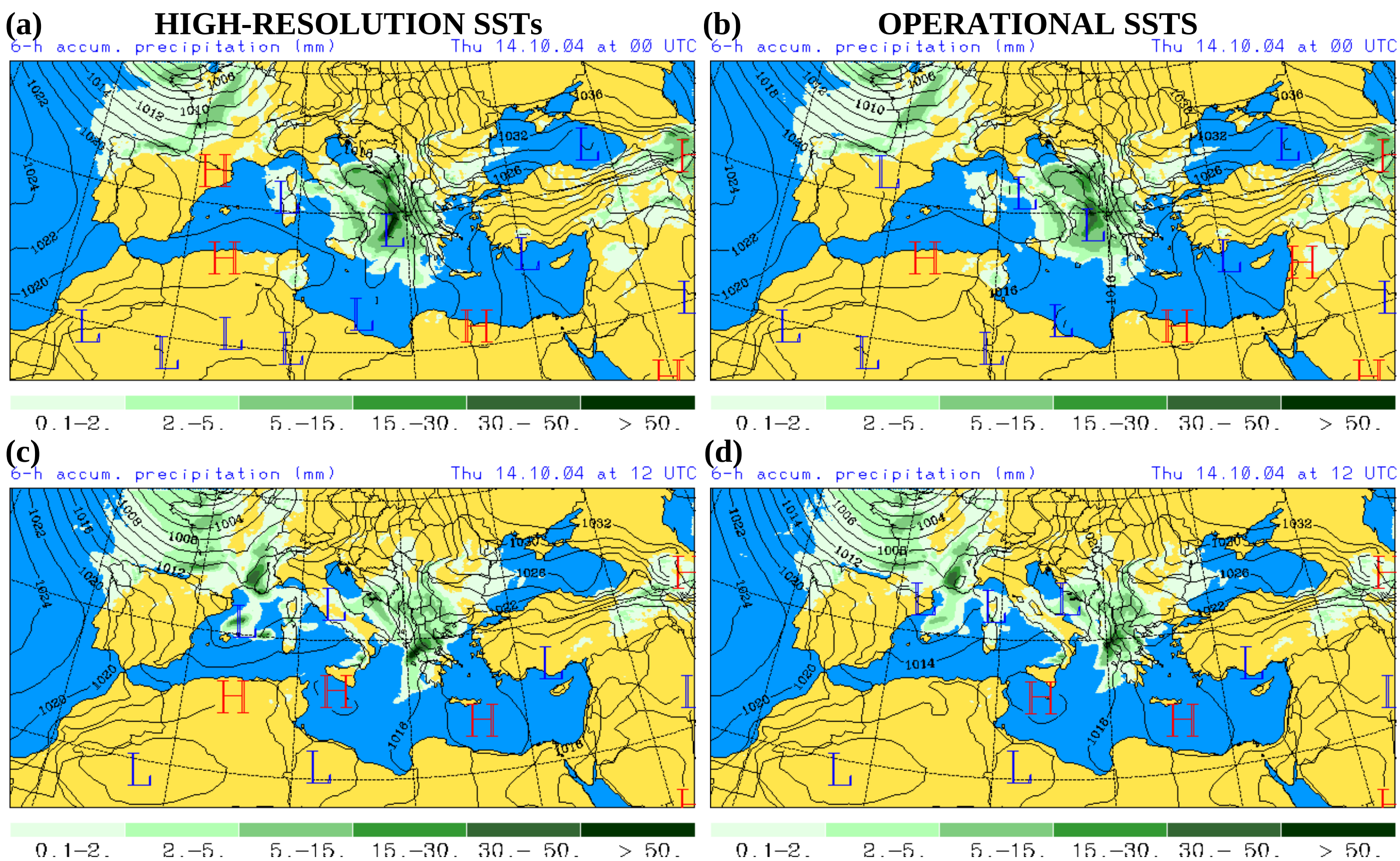

Figure 10. *Horizontal plots of 6-hrs total accumulated precipitation (mm) with the predicted mean sea-level pressure (hPa) overplotted (contours) at a, b) T+24 and c, d) T+36. Initial time at 0000 UTC 13 October 2004. Panels a, c: run with high-resolution SSTs. Panels b, d: run with operational SSTs. The valid time is indicated above each panel.*

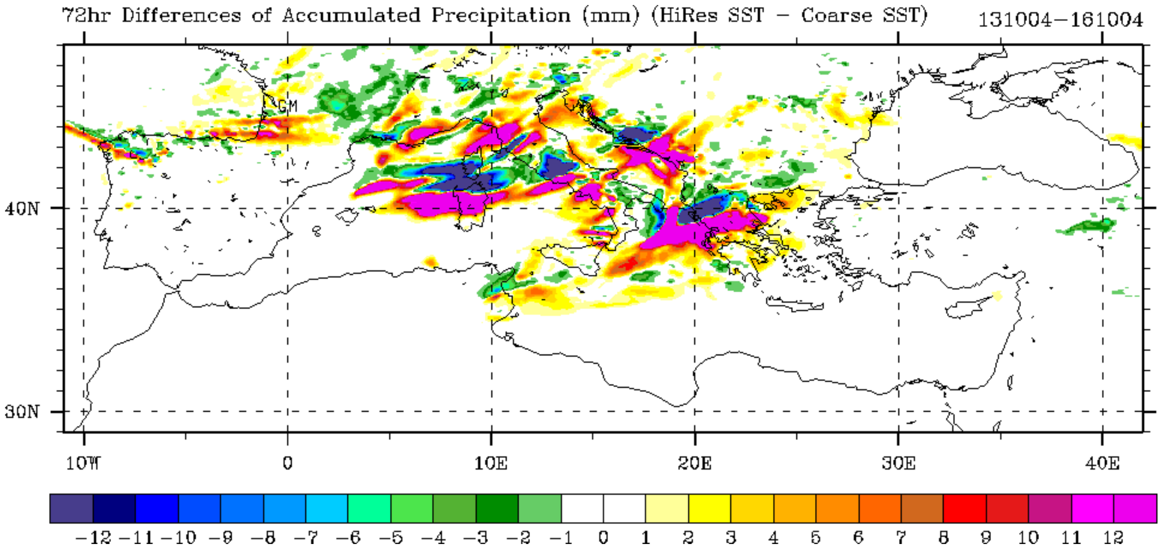

Figure 11. *The differences of the 72-hour accumulated precipitation (mm) between the SKIRON/Eta runs with the high-resolution and the operational SSTs. Initial time at 0000 UTC 13 October2004.*

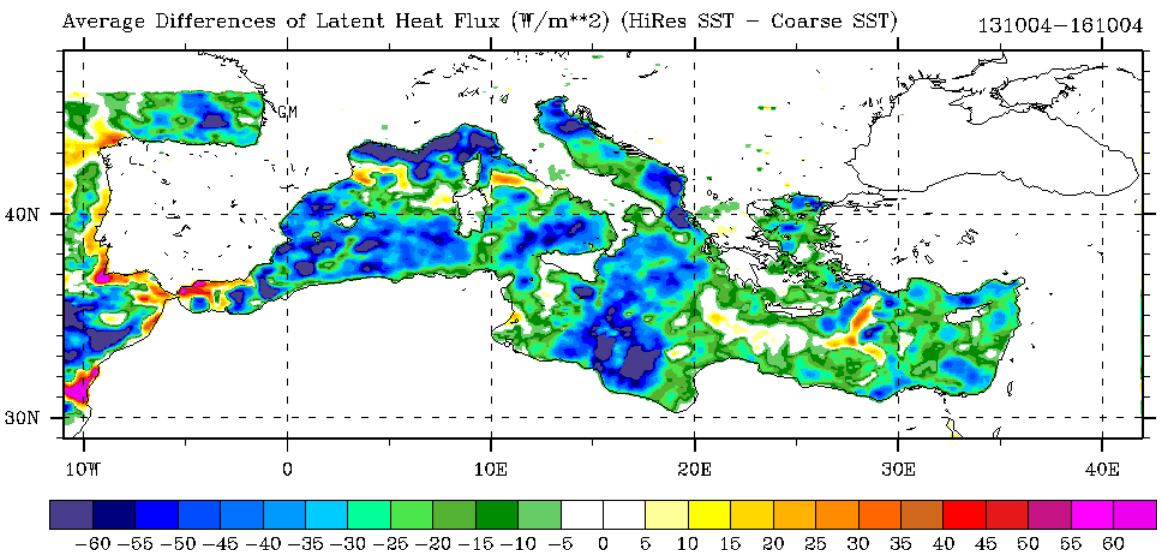

Figure 12. *The differences of the 72-hour average surface latent heat flux (W m^{-2}) between the SKIRON/Eta runs with the high-resolution and the operational SSTs. Initial time at 0000 UTC 13 October 2004. Negative (positive) values indicate stronger upward fluxes in the run with the high-resolution (operational) SSTs.*

The effects of the high-resolution SSTs on the model prediction at two coastal meteorological stations of western Greece, at Corfu (39° 37'N, 19° 55'E) and at Aktio (38° 57'N, 20° 47'E), are presented in Figures 13 and 14. The model predicted the magnitude and the temporal evolution of the 10m wind speed in good agreement with the observations. Especially at Corfu station the model captured the wind speed maximum which is probably attributed to mesoscale circulations and is generally difficult to be predicted. As far as the precipitation is concerned, the model generally overestimated its magnitude in both runs. It is not easy to conclude which model run provided the best precipitation forecasts because the operational SST run was closer to observations at Aktio while the high-resolution SST run was closer to observations at Corfu. However, the run with the operational SSTs seems to provide a better representation of the temporal evolution of the precipitation.

In conclusion, in this case study the different SSTs seem to influence the atmospheric flow at local scale, but the high-resolution dataset did not provide a clear improvement in the model forecasts.

(a) **(b)**

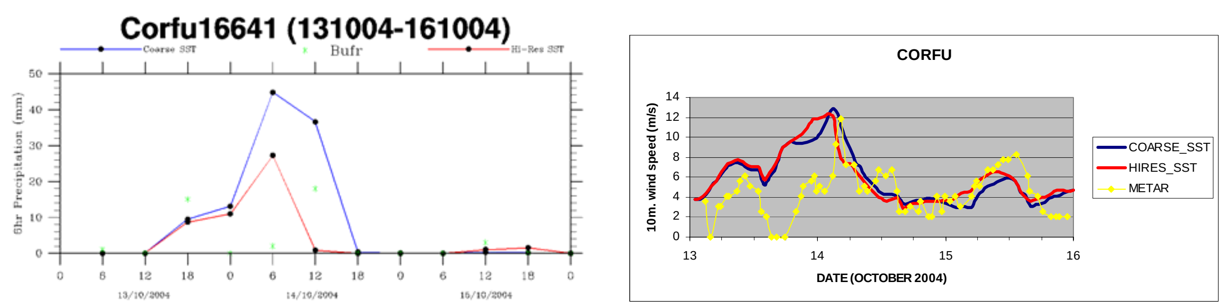

Figure 13. *Timeseries of a) the 6-hours accumulated precipitation (mm) and b) the 10m wind speed (m/s) at Corfu in the period 13 to 16 October 2004. Red line: SKIRON/Eta run with the high-resolution SSTs, Blue line: SKIRON/Eta run with the operational SSTs, Yellow line and Green dots: observations.*

(a) **(b)**

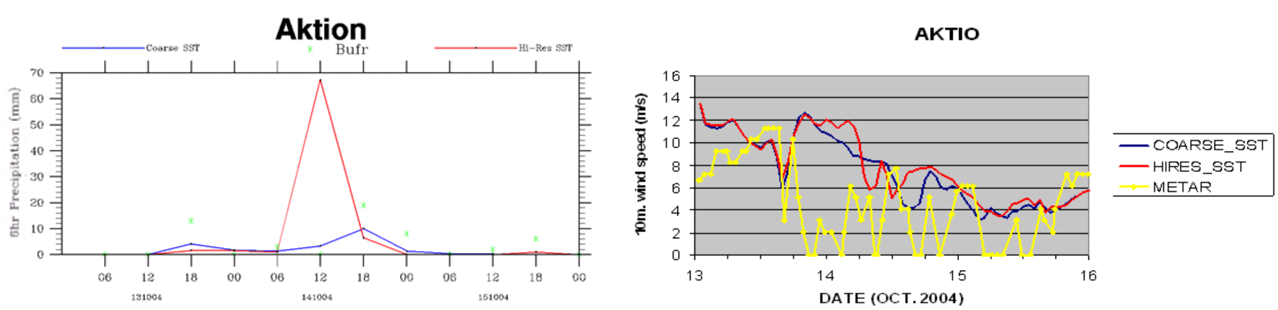

Figure 14. *Timeseries of a) the 6-hours accumulated precipitation (mm) and b) the 10m wind speed (m/s) at Aktio in the period 13 to 16 October 2004. Red line: SKIRON/Eta run with the high-resolution SSTs, Blue line: SKIRON/Eta run with the operational SSTs, Yellow line and Green dots: observations.*

4.1.2 Cyclone over Central Mediterranean

A sub-synoptic cyclone formed over central Mediterranean, south of Sicily, on 3 November 2004. Heavy precipitation and strong winds were reported from the nearby meteorological stations of Sicily. Moreover, large differences up to 1.5-2°C appeared between the high-resolution and the operational SSTs in this region on that day (Figure 8d). These conditions offered the chance of investigating the influence of the high-resolution SSTs on atmospheric flow patterns.

The cyclone formed over the sea southwest of Sicily at about 0600 UTC on 3 November. The formation took place in a wider region of low pressures (Figure 15a) due to the interaction of a low-level baroclinic zone with an upper-level cut-off low that was associated with cold air-masses. The interaction was intensified by the presence of low-static-stability air below the cut-off low. A closed circulation appeared in the United Kingdom Meteorological Office (UKMO) mean sea-level pressure charts at 1200 UTC (Figure 15b). The above development mechanisms together with the satellite signature of the system at 0000 UTC on 4 November (Figure 16) and the fact that it exhibited a warm-core at about 850 hPa (not shown) indicated a resemblance to the polar lows that form in northern Europe and sometimes in the Mediterranean. Further analysis is needed in order to establish this resemblance, but it is beyond the scope of this report.

The formation of the cyclone was predicted by SKIRON/Eta model in both simulations (with the high-resolution and the operational SSTs). A deeper cyclone was predicted in the hindcasts with the high-resolution SSTs (Figure 17) in agreement with the fact that the high-resolution SSTs were warmer than the operational ones on 3 November 2004 (Figure 8d). Mean sea-level pressure differences up to 1.8 hPa were exhibited between the two runs in the first 48 hours (Table 3). The comparison of the UKMO analyses (Figure 15) with the SKIRON/Eta forecasts (Figure 17) shows that the model predicted the cyclogenesis and the track of the system successfully in both runs. The model seems to overestimate the cyclone's deepening in the initial 24-30 hours, with the mean sea-level pressure in the operational SSTs run to be closer to the UKMO analyses. The difference between the predicted and the analyzed minimum mean sea-level pressure is likely to be due a) to model spin-up that was stronger in the run with the (warmer) high-resolution SSTs and/or b) to errors in the Meteo-France analysis because of data unavailability from the sparse observational network of that region. The data unavailability also may have resulted to an underestimation of the strength of the cyclone in the UKMO analysis charts of Figure 9.

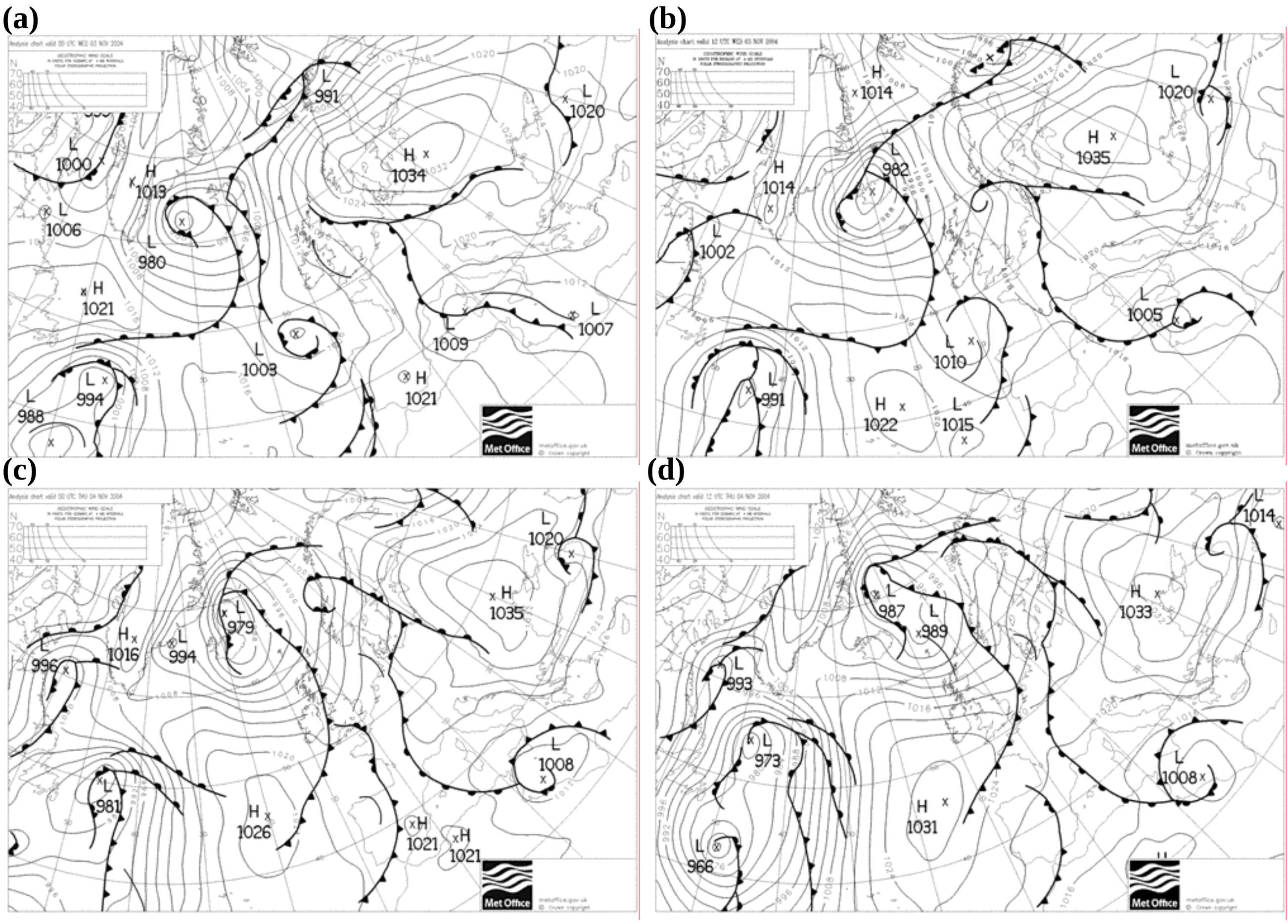

__Figure 15.__ UKMO mean sea-level pressure (hPa) analysis charts at a) 0000 UTC 3 November 2004, b) 1200 UTC 3 November 2004, c) 0000 UTC 4 November 2004, and d) 1200 UTC 4 November 2004.

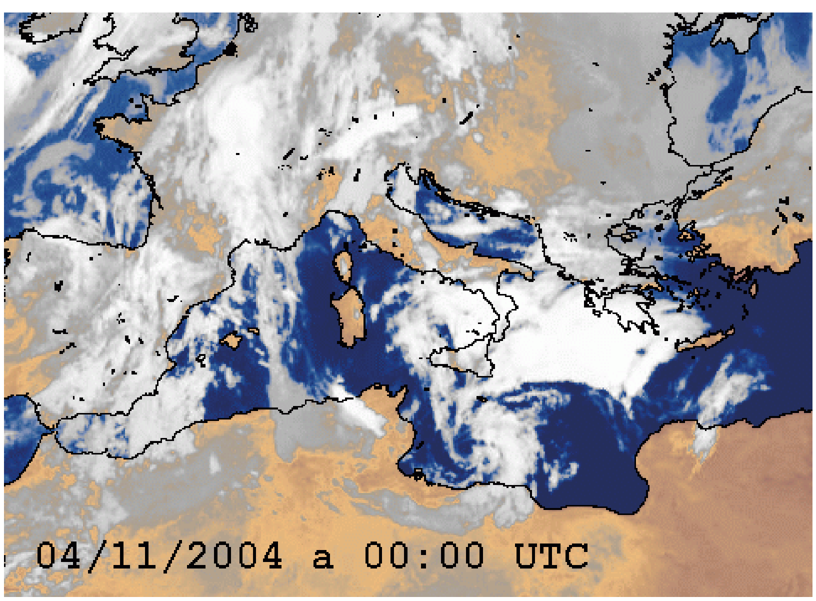

__Figure 16.__ Composite METEOSAT satellite image at 0000 UTC on 4 November 2004. (Source: MeteoFrance)

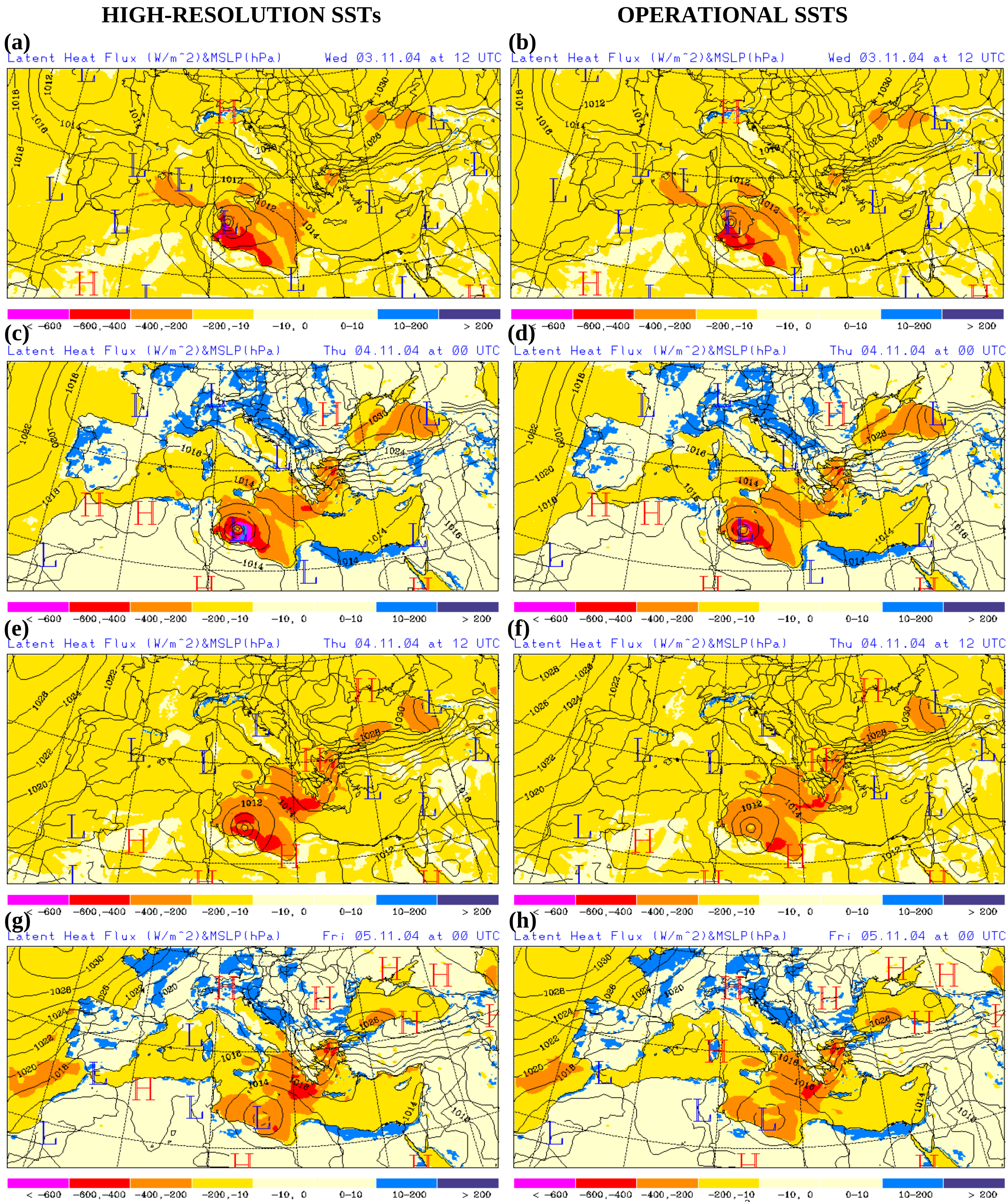

Figure 17. *Horizontal plots of SKIRON/Eta predicted surface latent heat flux (W m^{-2}) with the predicted mean sea-level pressure (hPa) overplotted (contours) at a, b) T+12, c, d) T+24, e, f) T+36, and g, h) T+48. Initial time at 0000 UTC 3 November 2004. Panels a, c, e, g: run with high-resolution SSTs. Panels b, d, f, h: run with operational SSTs. Negative values of latent heat flux correspond to upward fluxes.*

Valid Date	Forecast Time (hrs)	Minimum Mean Sea-Level Pressure (hPa)		
		UKMO analysis	SKIRON/Eta High-resolution SSTs	SKIRON/Eta Operational SSTs
0600 UTC 3/11/04	6		1001.4	1001.8
1200 UTC 3/11/04	12	1005	999.9	1000.4
1800 UTC 3/11/04	18		1000.7	1001.3
0000 UTC 4/11/04	24	1008	1001.3	1002.4
0600 UTC 4/11/04	30		1002.9	1004.7
1200 UTC 4/11/04	36	1008	1005.3	1007.0
1800 UTC 4/11/04	42		1008.0	1009.7
0000 UTC 5/11/04	48	1011	1008.7	1010.3

Table 3. *The mean sea-level pressure of the depression in the UKMO analyses and in the SKIRON/Eta runs with the high-resolution and the operational SSTs from 0000 UTC 3 November 2004 to 0000 UTC 5 November 2004.*

In agreement with the mean sea-level pressure, the 10m winds were predicted to be stronger in the run with the high-resolution SSTs (Figure 18). 10m wind speed up to about 19-20 m/s was predicted close to the center of the cyclone at T+18 in the run with the high-resolution SSTs, while in the operational SSTs run the maximum wind speed was generally weaker by 1-2 m/s. However, the location of the maximum 10m wind speed and the pattern of the wind field were similar in the two runs.

Significant differences appeared between the two runs in the precipitation field. Figure 19 shows that the two SST fields induced a different evolution in the rainbands associated with the depression. Heavier precipitation was predicted to fall close to the centre of the cyclone in the run with the high-resolution SSTs than in the operational SSTs run, while the opposite was predicted at larger distances.

The effects of the different SSTs in the evolution of the cyclone can be understood by examining the surface fluxes in its vicinity. Figure 17 illustrates the predicted instantaneous surface latent heat fluxes at 12-hourly intervals from T+12 to T+48, while Figure 20 presents the differences in the 72-hour average latent heat fluxes between the two runs. Strong upward latent and sensible (not shown) heat fluxes in excess of 400 or even 600 W/m^2 were predicted in the vicinity of the cyclone in both runs (Figure 17). However, stronger fluxes, with differences larger than 60 W/m^2, were predicted when the (warmer) high-resolution SSTs were used (Figure 20).

HIGH-RESOLUTION SSTs **OPERATIONAL SSTS**

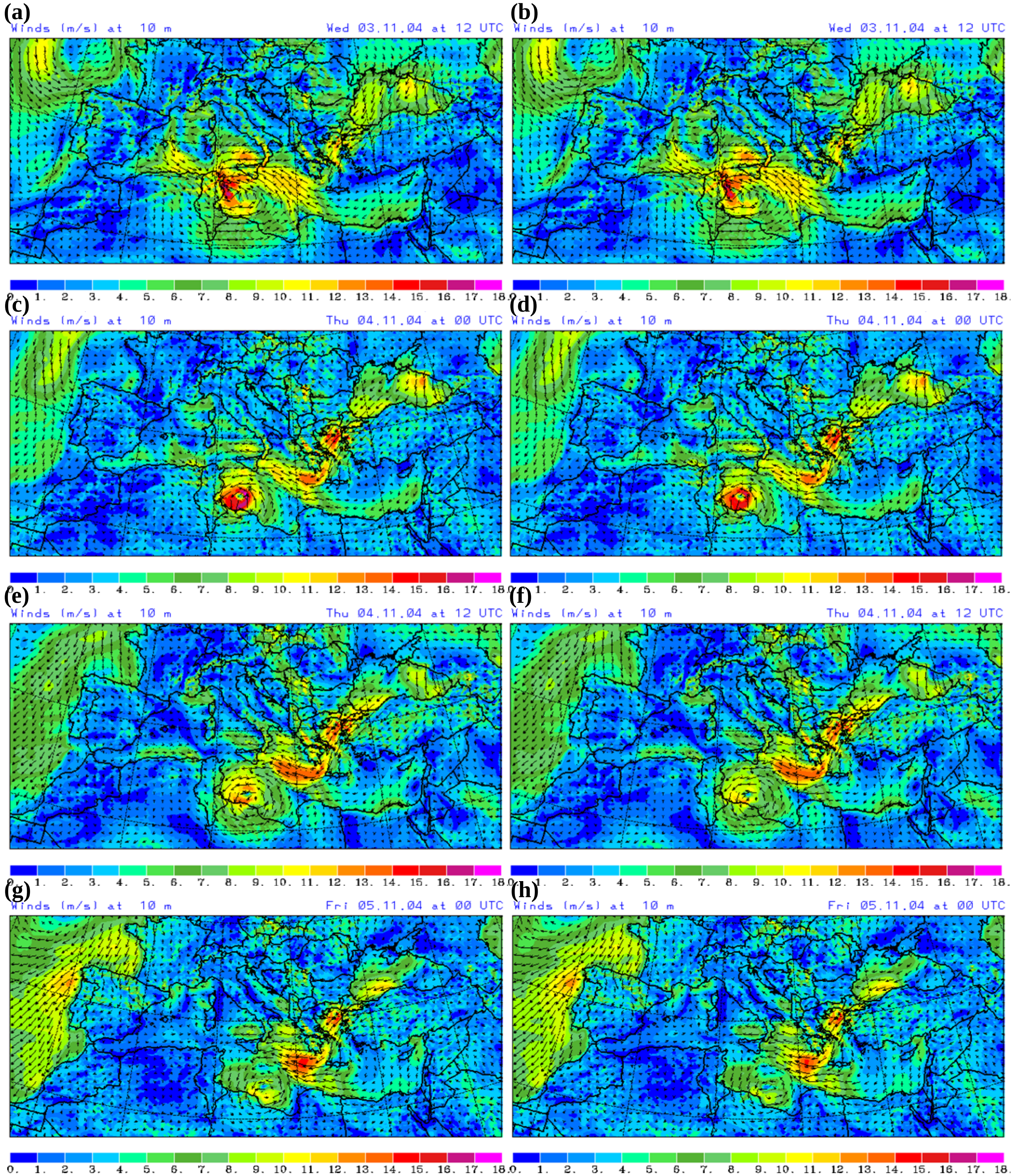

Figure 18. *Horizontal plots of SKIRON/Eta predicted 10m wind speed (m s^{-1}) and direction at a, b) T+12, c, d) T+24, e, f) T+36, and g, h) T+48. Initial time at 0000 UTC 3 November 2004. Panels a, c, e, g: run with high-resolution SSTs. Panels b, d, f, h: run with operational SSTs.*

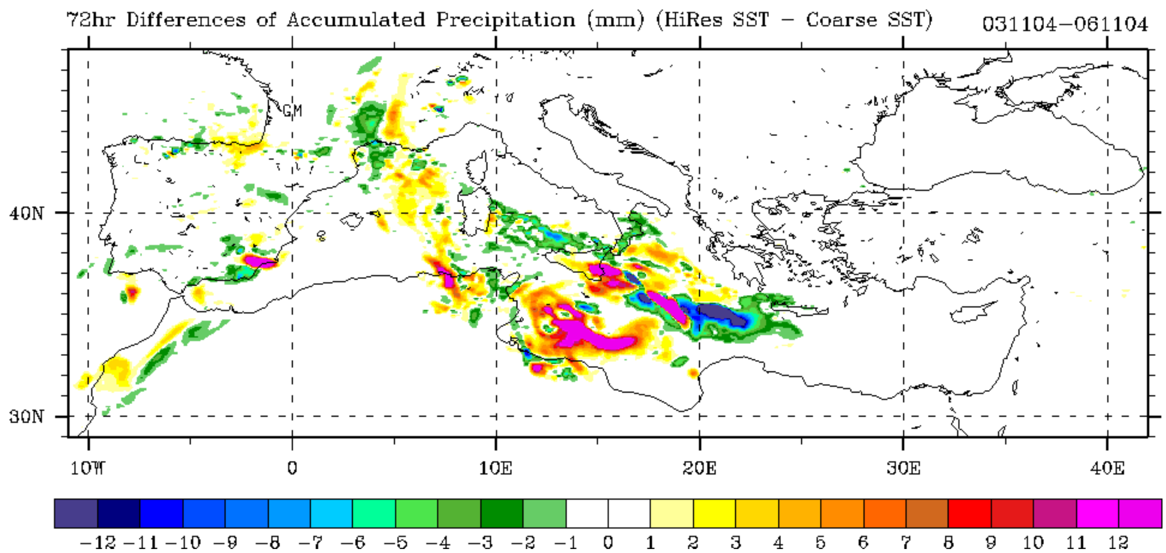

Figure 19. *The differences of the total 72-hour accumulated precipitation (mm) between the SKIRON/Eta runs with the high-resolution and the operational SSTs. Initial time at 0000 UTC 3 November 2004. Positive values indicate stronger precipitation in the run with the high-resolution SSTs.*

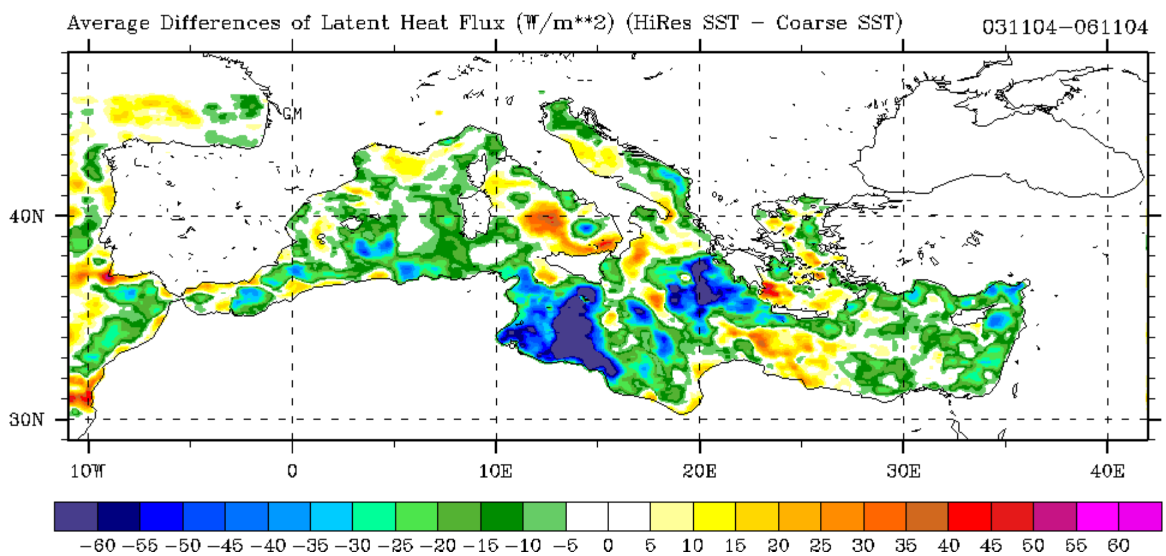

Figure 20. *The differences of the 72-hour average surface latent heat flux (W m^{-2}) between the SKIRON/Eta runs with the high-resolution and the operational SSTs. Initial time at 0000 UTC 3 November 2004. Negative (positive) values indicate stronger upward fluxes in the run with the high-resolution (operational) SSTs.*

The sensible and latent heat fluxes from the sea-surface depend on the surface wind speed and the thermodynamic disequilibrium between the sea-surface and the boundary layer, and they govern the latent heat release in the free troposphere. The surface fluxes increase the boundary layer θ_e and thus strengthen the convective activity of the storm. If this happens in an environment with small Rossby radius of deformation the temperature of the cyclone's core will increase and the central pressure of the cyclone will deepen. In turn, the lower surface pressure of the cyclone will lead to stronger radial pressure gradients and thus in stronger surface winds. Hence a positive feedback is established and the cyclone intensifies. This is the basis of the Wind-Induced Surface Heat Exchange mechanism that was proposed by Emanuel (1986) in order to explain the development of tropical cyclones and polar lows.

In this case study, the warmer SSTs that existed below the cyclone in the high-resolution SST run resulted in stronger thermodynamic disequilibrium in the boundary layer and thus in stronger fluxes of heat and moisture than in the run with the operational SSTs. Therefore, according to the above mechanism the development of a deeper cyclone in the high-resolution SST run is explained. As far as the cyclogenesis is concerned, it was mainly attributed to baroclinic instability and therefore it was similarly well-predicted in both runs.

4.1.3 Summary

The above case studies showed that the short to medium range forecasts are sensitive to changes in the underlying SST field in the presence of strong synoptic or mesoscale flow. The SKIRON/Eta predictions did not always seem to improve due to the use of the high-resolution satellite SST product of WP3. The influence of the fine-resolution information of the satellite SSTs on the model predictability and on our understanding of the atmospheric flow will be investigated further in the following section through statistical analysis.

4.2 Statistical analysis

The assessment of the influence of sharp SST gradients on the atmospheric flow regimes was performed with the use of well-known and widely accepted statistical methods. In this task the maximum available near shore surface observations have been used. The surface stations that provide operational surface observations (METAR and SYNOP) in the coastal Mediterranean areas are depicted in Figure 21. The data measurements are kindly provided from ECMWF.

The methodology of statistical analysis allows the examination of the model response in the quality of lower boundaries conditions providing significant conclusions about the impacts of high-resolution SST forcing in models’ forecasting capabilities.

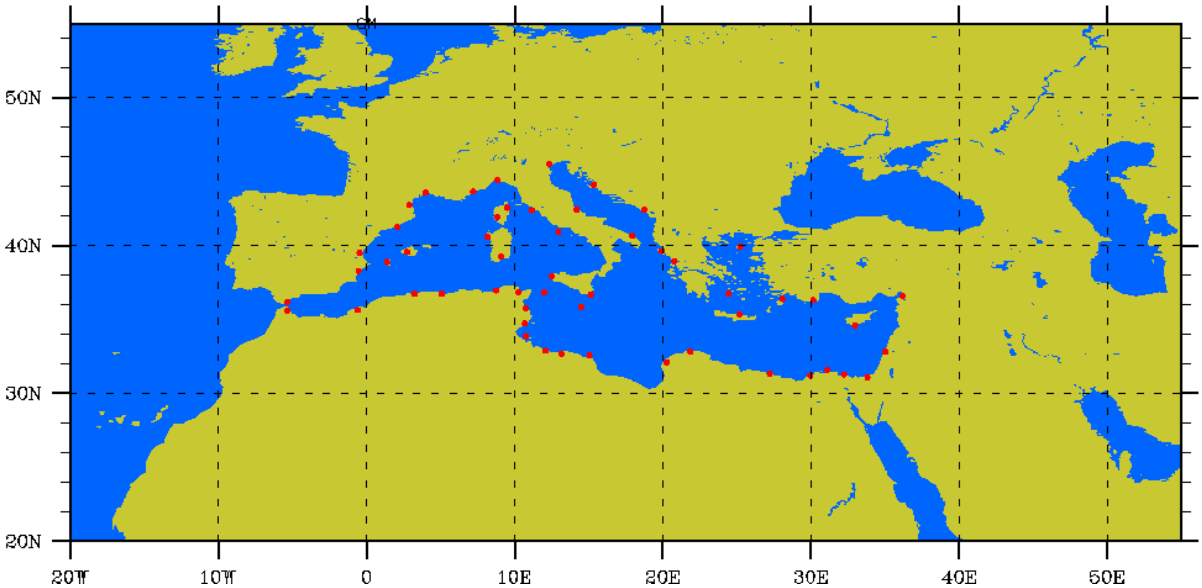

Figure 21. *The network of the coastal surface weather stations that provide observations to the Global Telecommunication System in our area of interest.*

Figure 22 shows the scatter diagrams of 10 m wind speed for 1 summer and 2 transient periods of 2004. The blue and red dots correspond to the forecasted values from Skiron/Eta integrations forced by the operational (low-resolution) and high-resolution SSTs, respectively, while their positions on the X/Y plot are depending on the relevant observed values. The scatter diagrams of wind speed along with the relevant regression lines did not show any significant modification between the model experiments forced by low and high resolution SSTs.

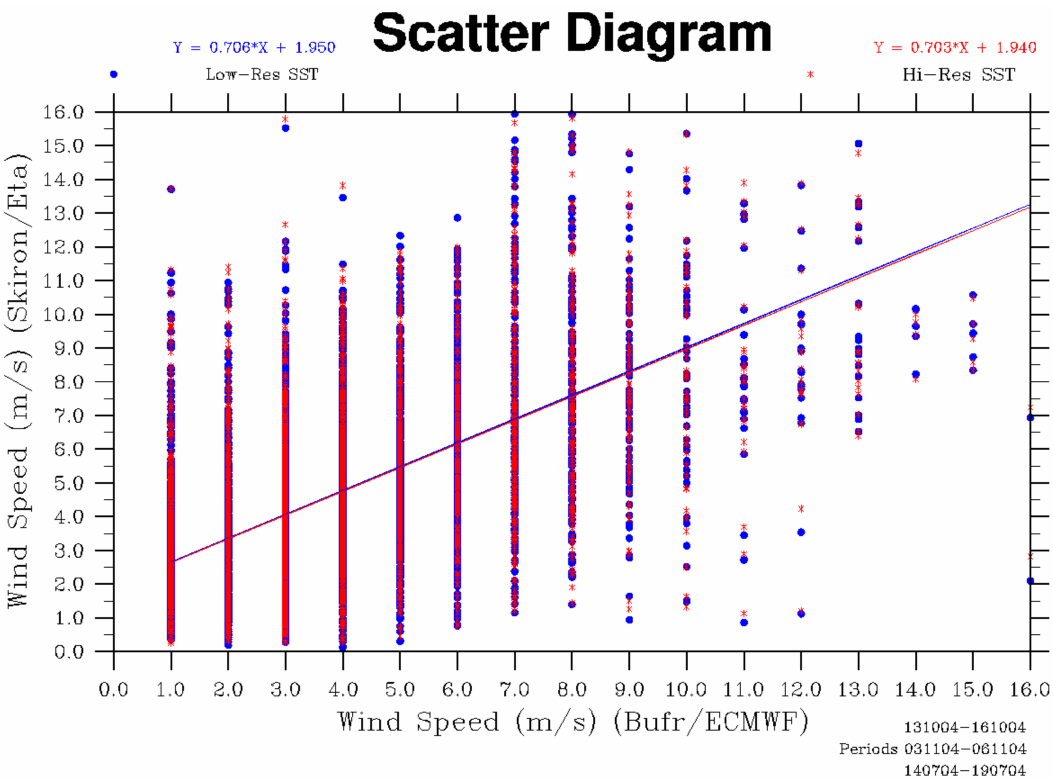

Figure 22. *Scatter diagrams of forecasted and observed 10m wind speed in m/s. The blue dots correspond to the simulations with low-resolution SST while the red dots to the relevant simulations with high-resolution SST.*

Figures 23a and b depict the 10 m wind speed bias and RMSE scores respectively. The periods of the simulations were similar to the abovementioned and the scores were computed with the time increment of 3 hours and for the 72 hours into forecast. According bias and RMSE scores, the differences in model response from the lower boundary forcing does not significantly affect its forecasting capabilities. In more details, a slight deviation between the two curves is mainly detected at the second day of the simulations but it didn't exceed the 0.25 m/s for bias and RMSE scores. The experiments with high-resolution SST exhibited a negligible increase of both scores during the specific period. It is also noteworthy that the model outputs showed a slight overestimation of the wind speed while the forecasted error was varied from 2.4-3.0 m/s. Despite the initial 12 hours of simulations (model spin up period) the model on both configurations showed significant consistency for the rest time into forecast.

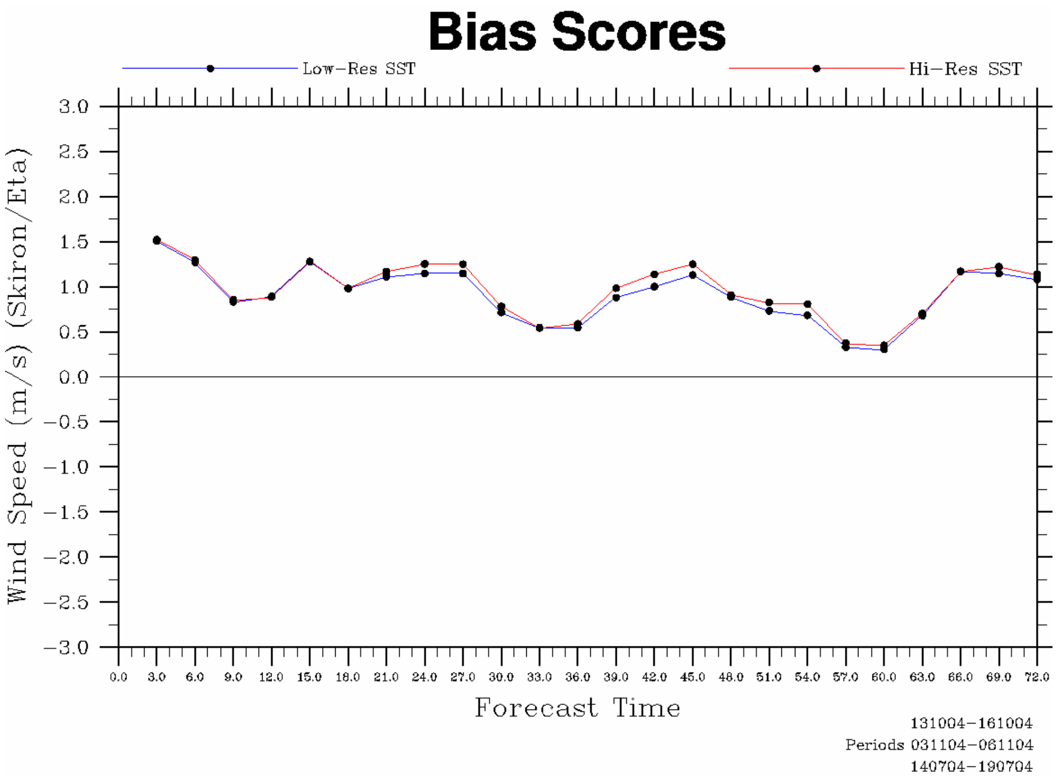

Figure 23a. *Bias scores referenced to the 10m wind speed for simulations forced by low-resolution SST (blue line) and high-resolution SST (red line).*

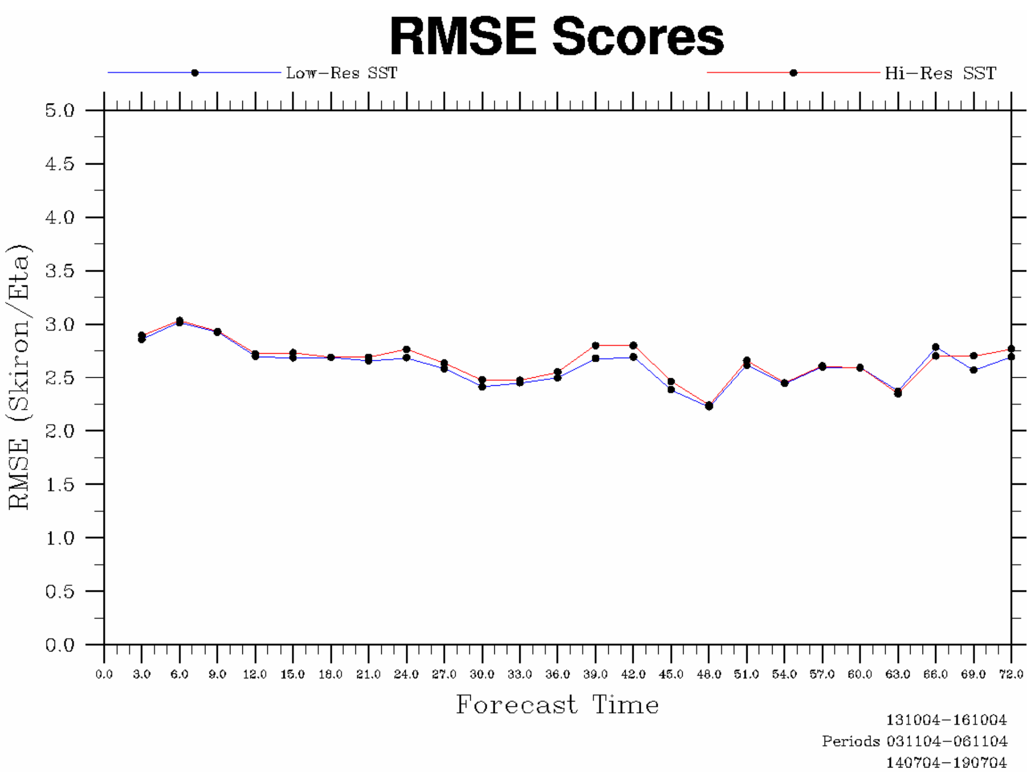

Figure 23b. *RMSE scores referenced to the 10m wind speed for simulations forced by low-resolution SST (blue line) and high-resolution SST (red line).*

The simulations with high-resolution SST indicated a significant improvement for both scores of near surface air temperature (Figures 24a and b). The reduction of RMSE can be characterized as systematic affecting the whole period of forecast (72 hours). However, in both experiments, with low and high resolution SST, there is a slight underestimation of the temperature which is turned into overestimation during the nocturnal periods. These periods are also characterized by the RMSE enhancement. Similar to the wind speed relevant scores, there is a significant consistency of bias and RMSE for the whole of the 72 hours forecast period.

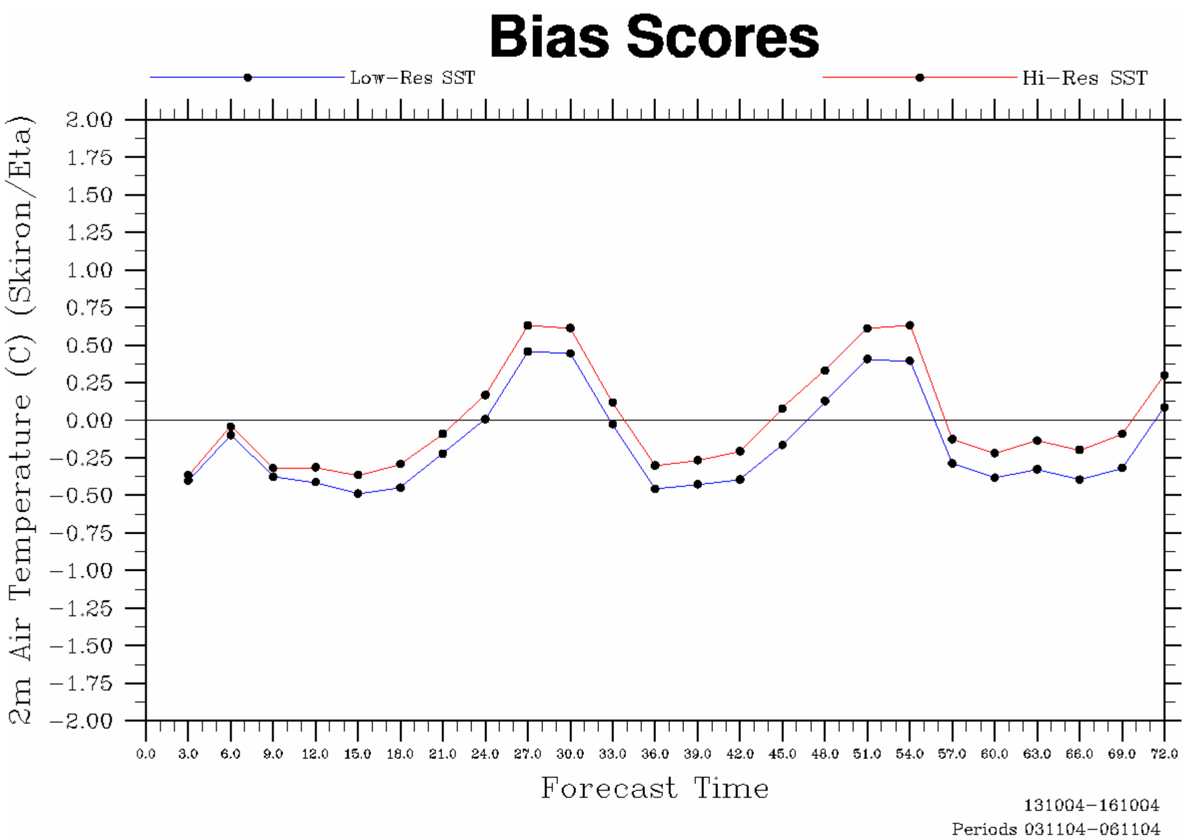

Figure 24a. *Bias scores referenced to the 2m air temperature for simulations forced by low-resolution SST (blue line) and high-resolution SST (red line).*

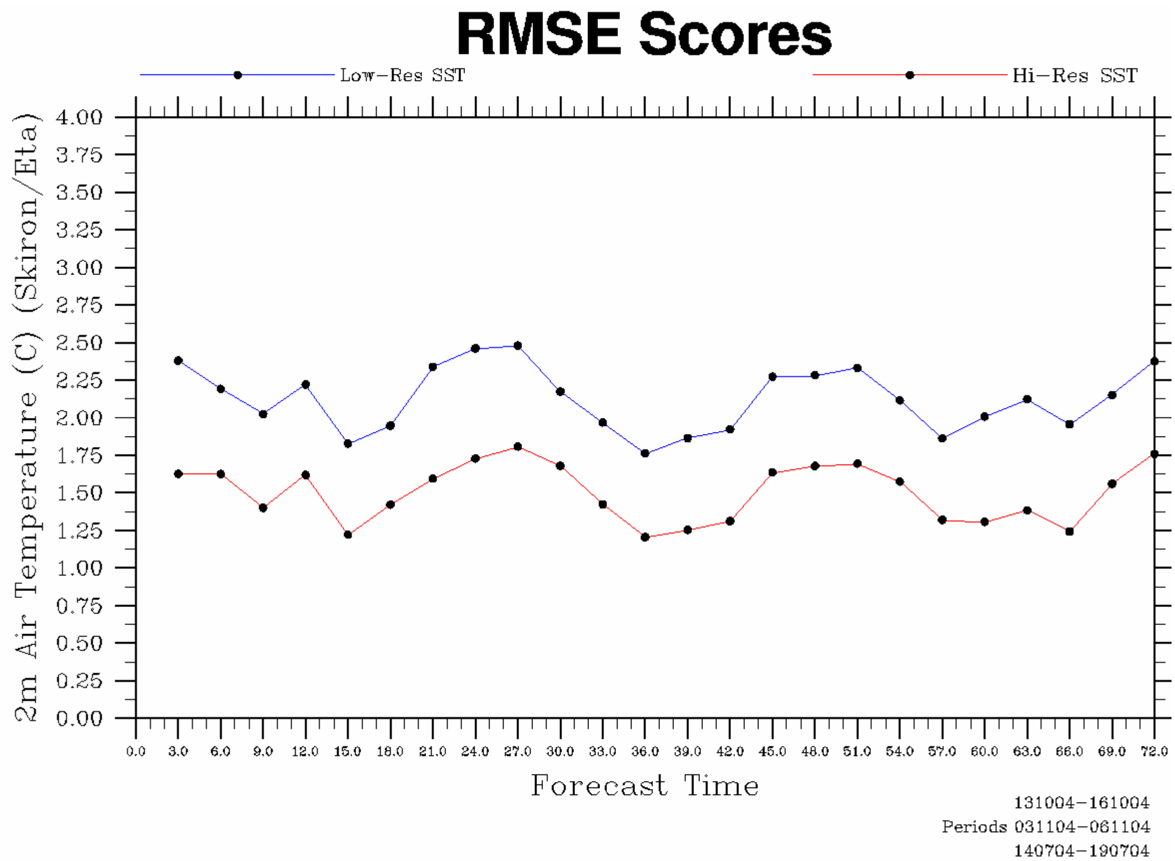

Figure 24b. *RMSE scores referenced to the 2m air temperature for simulations forced by low-resolution SST (blue line) and high-resolution SST (red line).*

The 6-hour accumulated precipitation scores for 7 discrete thresholds are depicted in Figures 25a and b. The bias and RMSE scores indicated that the forecasted precipitation is independent from the lower boundary forcing over the water bodies of the model. In more details, precipitation amounts over the threshold of 10mm seem to be affected from the high-resolution SST forcing. Nevertheless the sample of 15 measurements can not be considered as statistical significant and it can not act as an indicator of model performance. Therefore the simulated rain patterns are not influenced from the implementation of high resolution SST during the specific experiments. In these cases, the model showed a slight underestimation for the lower and medium precipitation thresholds.

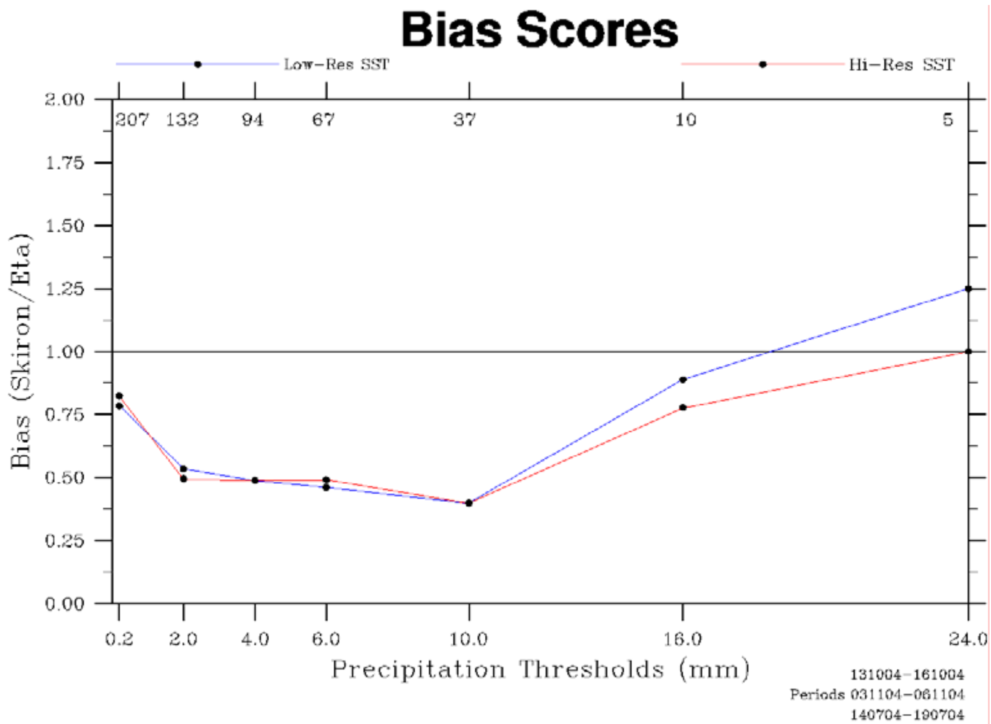

Figure 25a. *6-hour accumulated precipitation bias scores for 7 thresholds from 0.2 up to 24 mm. The blue line corresponds to the simulations forced by low-resolution SST and the red line to the simulations forced by high-resolution SST.*

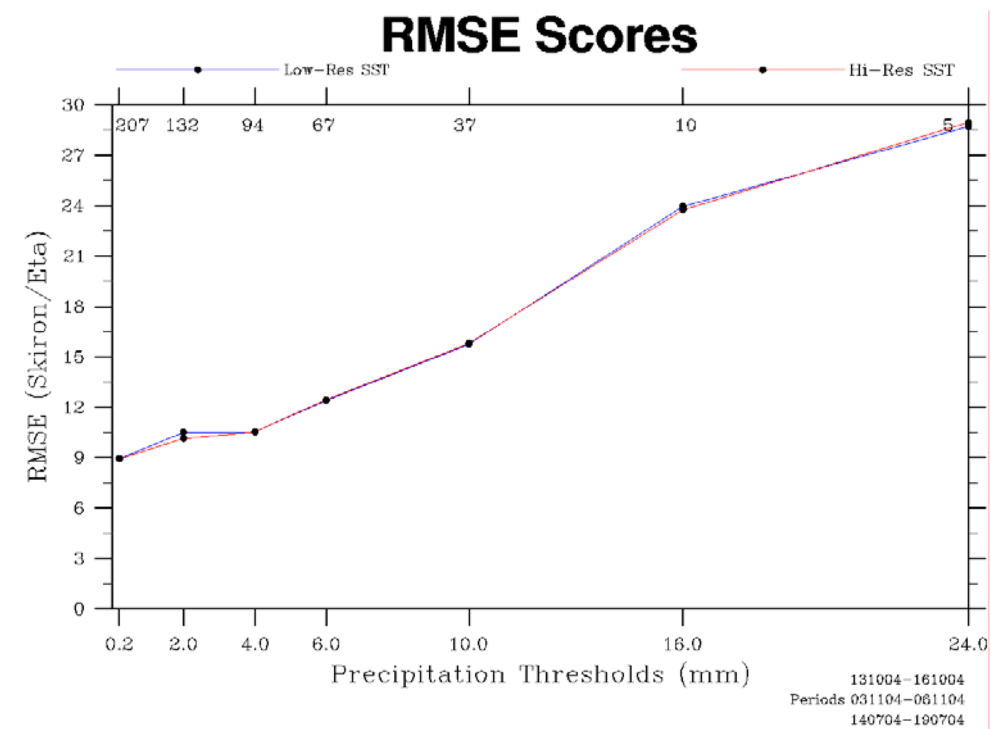

Figure 25b*. 6-hour accumulated precipitation RMSE scores for 7 thresholds from 0.2 up to 24 mm. The blue line corresponds to the simulations forced by low-resolution SST and the red line to the simulations forced by high-resolution SST.*

5. Conclusions

This study showed that the short to medium range forecasts are sensitive to changes in the underlying SST field in the presence of strong synoptic or mesoscale flow. However, the model predictions did not always seem to improve due to the use of the high-resolution satellite SST product of WP3.

In general the impacts of high-resolution SST forcing in Skiron/Eta performed simulations have been detected only to the 2m air temperature field. The forecasted accuracy of the specific field has been significantly improved while this low boundary forcing did not influence the wind speed and the precipitation forecasts. Of course there is no doubt that the implementation of high-resolution SST fields in atmospheric modeling causes the qualitatively improvement of the spatiotemporal distribution of the lower boundary conditions over the water bodies of the model domain. Whether such kind of forcing is also quantitatively detectable in the statistical scores of various fields is still a matter of further research.

References

Emanuel K.A. 1986: Air-Sea interaction theory for tropical cyclones. Part I.: Steady-State Maintenance. J. Atmos.Sci., **43**, 585-604.

Thiebaux, J., E. Rogers, W. Wang, and B. Katz, 2003: A new high-resolution blended real-time global sea surface temperature analysis. Bull. Amer. Meteor. Soc., **84**, 645-656.

Varinou M. 2000: Characteristic scales of dispersion and photochemical transformation of pollutants in Northeastern Mediterranean. PhD. Thesis, School of Physics, University of Athens, Greece. (in Greek)